SMAP Enhanced L1C Radiometer Half-Orbit 9 km EASE-Grid Brightness Temperatures, Version 3

USER GUIDE

How to Cite These Data

As a condition of using these data, you must include a citation:

Chaubell, J., S. Chan, R. S. Dunbar, J. Peng, and S. Yueh. 2020. *SMAP Enhanced L1C Radiometer Half-Orbit 9 km EASE-Grid Brightness Temperatures, Version 3*. [Indicate subset used]. Boulder, Colorado USA. NASA National Snow and Ice Data Center Distributed Active Archive Center. https://doi.org/10.5067/XB8K63YM4U8O. [Date Accessed].

FOR QUESTIONS ABOUT THESE DATA, CONTACT NSIDC@NSIDC.ORG

FOR CURRENT INFORMATION, VISIT https://nsidc.org/data/SPL1CTB_E

National Snow and Ice Data Center

TABLE OF CONTENTS

1 DATA DESCRIPTION

1.1 Parameters

Brightness temperature (TB; given in kelvins), derived from interpolated Level-1B RFI-mitigated antenna temperatures (TA) using the Backus-Gilbert (BG) optimal interpolation method, are provided on the EASE-Grid 2.0 at 9-km resolution in three different equal-area projections: global cylindrical, Northern Hemisphere azimuthal, and Southern Hemisphere azimuthal.

Refer to the Appendix of this document for details on all parameters.

1.2 File Information

1.2.1 Format

Data are in HDF5 format. For software and more information, including an HDF5 tutorial, visit the HDF Group's HDF5 website.

1.2.2 File Contents

As shown in Figure 1, each HDF5 file is organized into the following main groups, which contain additional groups and/or data sets:

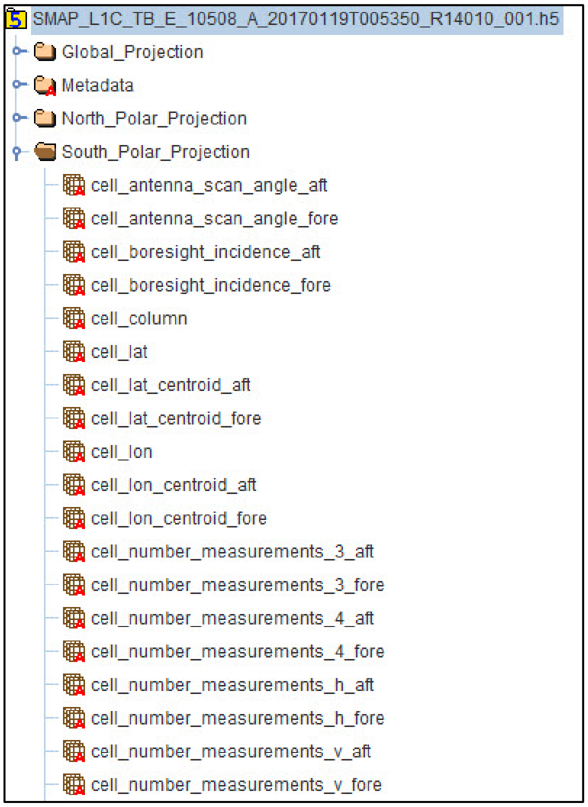

Figure 1. Subset of File Contents. For a complete list of file contents for the SMAP enhanced Level-1C brightness temperature product, refer to the Appendix.

1.2.3 Data Fields

Each file contains the main data groups summarized in this section. For a complete list and description of all data fields within these groups, refer to the Appendix of this document.

Data fields are stored as one-dimensional arrays of size *N*, where *N* is the number of valid cells covered by the radiometer swath on the grid. Note that *N* varies with projections, but remains the same for both fore-looking and aft-looking views within a given projection.

Global Projection

Contains data that represent fore- and aft-looking views of the 360° antenna scan, including brightness temperatures, instrument viewing geometry information, and quality bit flags.

Corrected brightness temperatures are also provided, such as *cell_tb_h_surface_corrected_aft* (as opposed to *cell_tb_h_aft).* For these brightness temperatures, an additional correction procedure has been applied to correct for emission due to water or land; see the *Water/Land Contamination Correction* section in the SPL1BTB User Guide for details. (Level-1B brightness temperatures are used as input for this product).

North Polar Projection

Contains the same data as the Global Projection group, but data are in the Northern Hemisphere azimuthal EASE-Grid 2.0 projection.

South Polar Projection

Contains the same data as the Global Projection groups, but data are in the Southern Hemisphere azimuthal EASE-Grid 2.0 projection.

1.2.4 Metadata Fields

Includes all metadata that describe the full content of each file. For a description of all metadata fields for this product, refer to the Product Specification Document (Chan & Dunbar, 2020).

1.2.5 File Naming Convention

Files are named according to the following convention:

```
SMAP_L1C_TB_E_[Orbit#]_[A/D]_yyyymmddThhmmss_RLVvvv_NNN.[ext]
```

For example:

```
SMAP_L1C_TB_E_10508_A_20170119T005350_R14010_001.h5
```

Table 1 describes the variables within a file name:

Table 1. File Naming Convention

<table>
<tr><th>Variable</th><th>Description</th></tr>
<tr><td>SMAP</td><td>Indicates SMAP mission data</td></tr>
<tr><td>L1C_TB_E</td><td>Indicates specific product (L1C: Level-1C; TB: Brightness Temperature; E: Enhanced)</td></tr>
<tr><td>[Orbit#]</td><td>5-digit sequential number of the orbit flown by the SMAP spacecraft when data were acquired. Orbit 00000 began at launch. Orbit numbers increment each time the spacecraft flies over the southernmost point in the orbit path.</td></tr>
<tr><td>[A/D]</td><td>Half-orbit pass of the satellite, such as:
A: Ascending (where satellite moves from South to North, and 6:00 p.m. is the local solar time)
D: Descending (where satellite moves from North to South, and 6:00 a.m. is the local solar time)</td></tr>
<tr><td>yyyymmddThhmmss</td><td>Date/time in Universal Coordinated Time (UTC) of the first data element that appears in the product, where:
<table>
<tr><td>yyyymmdd</td><td>4-digit year, 2-digit month, 2-digit day</td></tr>
<tr><td>T</td><td>Time (delineates the date from the time, i.e. yyyymmddThhmmss)</td></tr>
<tr><td>hhmmss</td><td>2-digit hour, 2-digit minute, 2-digit second</td></tr>
</table></td></tr>
<tr><td>RLVvvv</td><td>Composite Release ID, where:
<table>
<tr><td>R</td><td>Release</td></tr>
<tr><td>L</td><td>Launch Indicator (1: post-launch standard data)</td></tr>
<tr><td>V</td><td>1-Digit CRID Major Version Number (Note: the data set's major version does not necessarily coincide with the CRID major version)</td></tr>
<tr><td>vvv</td><td>3-Digit CRID Minor Version Number</td></tr>
</table>
Example: R13242 indicates a post-launch data product with a version of 3.242.
Refer to the SMAP Data Versions page for version information.</td></tr>
<tr><td>NNN</td><td>Number of times the file was generated under the same version for a particular date/time interval (002: 2nd time)</td></tr>
<tr><td>.[ext]</td><td>File extensions include:
<table>
<tr><td>.h5</td><td>HDF5 data file</td></tr>
<tr><td>.qa</td><td>Quality Assurance file</td></tr>
<tr><td>.xml</td><td>XML Metadata file</td></tr>
</table></td></tr>
</table>

1.3 Spatial Information

1.3.1 Coverage

Coverage spans from 180°W to 180°E, and from approximately 85.044°N and 85.044°S for the EASE-Grid, Version 2.0. The swath width is 1000 km, enabling nearly global coverage every two to three days. Figure 2 shows the spatial coverage of the SMAP L-Band Radiometer for one descending half orbit, which comprises one file of this data set.

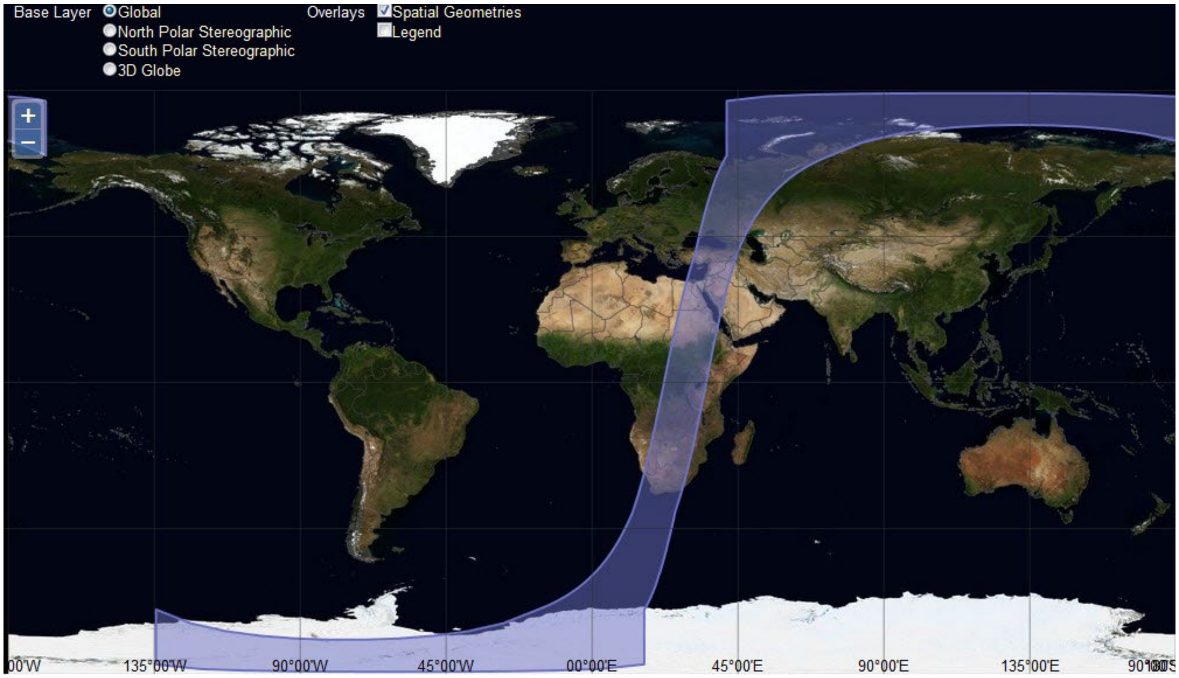

Figure 2. Spatial coverage map displaying one descending half orbit of the SMAP L-Band Radiometer.

1.3.2 Resolution

The native spatial resolution of the radiometer footprint is approximately 36 km. Data are then interpolated using the Backus-Gilbert optimal interpolation algorithm on the global cylindrical, Northern Hemisphere azimuthal, and Southern Hemisphere azimuthal EASE-Grid 2.0 projections with 9 km grid resolution.

1.3.3 Geolocation

These data are provided on the EASE-Grid 2.0 in three different equal-area projections: a global cylindrical, a Northern Hemisphere azimuthal, and Southern Hemisphere azimuthal. Each grid cell has a nominal area of approximately 9 x 9 km^2 regardless of longitude and latitude. The following tables provide information for geolocating this data set. For more on EASE-Grid 2.0, refer to the EASE Grids website.

Table 2. Geolocation details for the EASE-Grid 2.0 projections used in this product

	Global	Northern Hemisphere	Southern Hemisphere
Geographic coordinate system	WGS 84	WGS 84	WGS 84
Projected coordinate system	EASE-Grid 2.0 Global	EASE-Grid 2.0 North Azimuthal	EASE-Grid 2.0 South Azimuthal
Longitude of true origin	0	0	0
Standard Parallel	30° N	90° N	90° S
Scale factor at longitude of true origin	N/A	N/A	N/A
Datum	WGS 84	WGS 84	WGS 84
Ellipsoid / spheroid	WGS 84	WGS 84	WGS 84
Units	meter	meter	meter
False easting	0	0	0
False northing	0	0	0
EPSG code	6933	6931	6932
PROJ4 string	+proj=cea +lon_0=0 +lat_ts=30 +x_0=0 +y_0=0 +ellps=WGS84 +towgs84=0,0,0,0,0,0,0 +units=m +no_defs	+proj=laea +lat_0=90 +lon_0=0 +x_0=0 +y_0=0 +ellps=WGS84 +towgs84=0,0,0,0,0,0,0 +units=m +no_defs	+proj=laea +lat_0=-90 +lon_0=0 +x_0=0 +y_0=0 +ellps=WGS84 +towgs84=0,0,0,0,0,0,0 +units=m +no_defs
Reference	http://epsg.io/6933	http://epsg.io/6931	http://epsg.io/6932

Table 3. Grid details for the EASE-Grid 2.0 projections used in this product

	Global	Northern Hemisphere	Southern Hemisphere
Grid cell size (x, y pixel dimensions)	9,008.05 m (x) 9,008.05 m (y)	9,000 m (x) 9,000 m (y)	9,000 m (x) 9,000 m (y)
Number of columns	3,856	2,000	2,000
Number of rows	1,624	2,000	2,000
Geolocated lower left point in grid	85.044° S, 180.000° W	84.634050° S, 45.000000° W	84.634050° N, 135.000000° W
Nominal gridded resolution	9 km by 9 km	9 km by 9 km	9 km by 9 km
Grid rotation	N/A	N/A	N/A
ulxmap – x-axis map coordinate of the outer edge of the upper-left pixel	-17367530.45	-9000000.0	-9000000.0
ulymap – y-axis map coordinate of the outer edge of the upper-left pixel	7314540.83	9000000.0	9000000.0

1.4 Temporal Information

1.4.1 Coverage

Coverage spans from 31 March 2015 to 04 December 2023.

1.4.2 Satellite and Processing Events

Due to instrument maneuvers, data downlink anomalies, data quality screening, and other factors, small gaps in the SMAP time series will occur. Details of these events are maintained on two master lists:

SMAP On-Orbit Events List for Instrument Data Users
Master List of Bad and Missing Data

A significant gap in coverage occurred between 19 June and 23 July 2019 after the SMAP satellite went into Safe Mode. A brief description of the event and its impact on data quality is available in the SMAP Post-Recovery Notice.

1.4.3 Latencies

FAQ: What are the latencies for SMAP radiometer data sets?

1.4.4 Resolution

Each enhanced Level-1C half-orbit file spans approximately 49 minutes. The SMAP orbit yields a 2-3 day average revisit frequency and repeats the exact swath every 8 days.

2 DATA ACQUISITION AND PROCESSING

This section has been adapted from the Algorithm Theoretical Basis Document (ATBD) for this product (Chaubell et al. 2018).

2.1 Background

The enhanced Level-1C brightness temperature product is an interpolated and gridded version of SMAP L1B Radiometer Half-Orbit Time-Ordered Brightness Temperatures, Version 5 and thus shares most of the same major output data fields, data granularity (one half-orbit per file), and theory of measurements. Refer to the Level-1B user guide for more details.

2.2 Instrumentation

For a detailed description of the SMAP instrument, visit the SMAP Instrument page at Jet Propulsion Laboratory (JPL) SMAP website.

2.3 Acquisition

Antenna temperatures from the baseline SMAP L1B Radiometer Half-Orbit Time-Ordered Brightness Temperatures, Version 5 (SPL1BTB) product are used as input to calculating this enhanced Level-1C brightness temperature product.

2.4 Derivation Techniques and Algorithms

2.4.1 Backus-Gilbert Optimal Interpolation Algorithm

The SMAP Level-1B brightness temperature product (SPL1BTB)—the input data for this product—contains calibrated, geolocated, time-ordered brightness temperatures acquired by the SMAP radiometer. The aim of this SMAP enhanced Level-1C brightness temperature product (SPL1CTB_E) is to provide an optimal interpolation of the radiometer measurements onto a global 9-km grid. The SMAP sampling pattern results in overlapping measurements which, together with optimal interpolation, results in a better utilization of the SMAP Level-1B brightness temperatures.

There are a number of algorithms directed towards the goal of image reconstruction and interpolation. A long-standing approach and one with extensive heritage in microwave radiometry is the Backus-Gilbert (BG) interpolation (Backus and Gilbert 1970). This technique has been applied to the Special Sensor Microwave/Imager (SSM/I) measurements (Stogryn, 1978; Poe, 1990; Robison et al., 1992; Farrar and Smith, 1992; Sethmann et al., 1994; Long and Daum, 1998; Migliaccio and Gambardella, 2005) and the Tropical Rainfall Measuring Mission (TRMM) Microwave Imager (TMI) measurements (Chakraborty et al., 2008). A unique feature of the BG interpolation is that it is optimal in the sense that the resulting interpolated data is closest to what would have been measured had the radiometer actually made the measurements with the interpolation point as its bore-sight center (Poe, 1990). In this sense and in this respect, it is superior to ad hoc or empirical interpolation techniques. According to Long and Brodzik (2016), BG provides higher spatial resolution surface brightness temperature images with smaller total error compared with conventional drop-in-the-bucket gridded image formation. The SPL1CTB_E algorithm uses the polarimetric implementation of the BG optimal interpolation algorithm derived by Dr. Simon Yueh to interpolate baseline SMAP Level-1B antenna temperatures on the EASE-Grid 2.0 points within the boundaries of the orbit path.

For details regarding the BG theory and implementation, refer to Section 2 of the enhanced Level-1B ATBD (Chaubell et al. 2016). The enhanced L1B product is not publicly distributed; it is strictly used for internal processing and generation of this enhanced Level-1C product.

2.4.2 Gridding Algorithm

As mentioned previously, the SPL1CTB_E algorithm uses BG optimal interpolation to interpolate SMAP Level-1B antenna temperatures on the EASE-Grid 2.0 points within the boundaries of the orbit path.

In other words, calling ρ_d a point on the EASE-Grid 2.0, the antenna temperature is computed at ρ_d as

$$T_A(\rho_d) = \sum_{i=1}^{N} a_i \cdot T_{A_i} \qquad \text{(Equation 1)}$$

where T_{A_i} are the antenna temperatures at the SMAP footprint locations ρ_d, i=1…N.

The coefficients are given by

$$\bar{a} = \bar{\bar{g}}^{-1} \cdot \bar{v} + \left(\frac{2-\bar{u}^T \cdot \bar{\bar{g}}^{-1} \cdot \bar{v}}{\bar{u}^T \cdot \bar{\bar{g}}^{-1} \cdot \bar{u}}\right) \cdot \bar{\bar{g}}^{-1} \cdot \bar{u} \qquad \text{(Equation 2)}$$

where the elements of the matrix g are

$$g_{im} = \sum_{j,k=1}^{4} \int dA G_{jk}(\bar{\rho}_i, \bar{\rho})\, G_{jk}(\bar{\rho}_m, \bar{\rho}) \qquad \text{(Equation 3)}$$

and the vectors $\bar{v}$ and $\bar{u}$ are given by

$$v_i = \sum_{j,k=1}^{4} \int dA G_{jk}(\bar{\rho}_i, \bar{\rho})\, G_{jk}(\bar{\rho}_d, \bar{\rho}) \qquad \text{(Equation 4)}$$

and

$$u_i = \int dA G_{11}(\bar{\rho}_i, \bar{\rho}) + G_{21}(\bar{\rho}_i, \bar{\rho}) + G_{12}(\bar{\rho}_i, \bar{\rho}) + G_{22}(\bar{\rho}_i, \bar{\rho})\ . \qquad \text{(Equation 5)}$$

These equations are the bases for the direct evaluation of the vectors $\bar{v}$ and $\bar{u}$ and the matrix g, necessary to obtain the coefficients $\bar{a}$. These calculations can be computationally very expensive. In order to make the algorithm more computationally efficient, some approximations were implemented. Details of these approximations and the corresponding error evaluation can be found in the enhanced Level-1B ATBD (Chaubell et al. 2016).

2.5 Processing

This enhanced Level-1C product is generated by the SMAP Science Data Processing System (SDS) at JPL in Pasadena, California USA. The processing software ingests a half-orbit file of the enhanced Level-1B radiometer brightness temperature data set to extract and transfer key data fields to the SPL1CTB_E product. Only cells that are covered by the actual swath for a given projection are written in the product.

Prior to the production of the SPL1CTB_E product, the enhanced Level-1B processor reads from the SPL1BTB product the baseline Level-1B antenna temperatures, which have been calibrated (by removing sun/moon/galactic contributions and applying reflector emissivity corrections) and processed by radio frequency interference detection and mitigation algorithms. Two-dimensional arrays that are transferred from the enhanced Level-1B are reformatted as one-dimensional arrays for compactness and improved input/output speed in Level-2 processing. The enhanced Level-1B algorithm applies the Backus-Gilbert interpolation to interpolate Level-1B antenna temperatures on the EASE-Grid 2.0 points within the boundaries of the orbit path. The algorithm uses six SMAP footprints from the baseline SPL1BTB product to perform the interpolation. The selection of those points is explained in the enhanced Level-1B ATBD (Chaubell et al. 2016). If one of those selected points is a fill value, then the value assigned to the antenna temperature is a fill value. The interpolated antenna temperatures are further processed to remove the effects of the antenna sidelobes outside the radiometer antenna main beam, cross-polarizations, Faraday rotation, and atmospheric effects (excluding rain). The resulting enhanced Level-1B data represent enhanced surface-referenced brightness temperatures.

2.6 Quality, Errors, and Limitations

2.6.1 Error Sources

This enhanced Level-1C brightness temperature product (SPL1CTB_E) contains a subset of data fields of the input enhanced Level-1B data set. In terms of noise performance, SPL1CTB_E inherits the same Error Sources that affect SPL1BTB. These error sources include RFI, radiometric noise and calibration error, modified by the process of Backus-Gilbert interpolation in enhanced L1B data. The interpolation process is not expected to affect the calibration errors, such as biases and drifts, but will reduce the radiometric noise, such as the random component of the brightness temperature error. Conversely, the interpolation process may enlarge the effective antenna pattern footprint of the brightness temperature measurement.

In addition, because image reconstruction includes a trade-off between noise and resolution, estimated noise variances in the interpolated fields are reported in the enhanced Level-1B ATBD

(Chaubell et al. 2016). However, the noise levels obtained for that product and thus in SPL1CTB_E measurements are improved over the baseline SPL1BTB single footprint measurements due to the interpolation performed, and are similar to the noise levels of the baseline SPL1CTB product, which also performs an interpolation of single footprint measurements in mapping to a 36 km grid.

For more information, please refer to the enhanced Level-1B ATBD (Chaubell et al. 2016).

2.6.2 Quality Assessment

For in-depth details regarding the quality of these data, refer to the Assessment Report (Peng et al. 2020).

2.6.3 Quality Overview

Each HDF5 file contains metadata with Quality Assessment (QA) metadata flags that are set by the SDS at the JPL prior to delivery to the National Snow and Ice Data Center Distributed Active Archive Center (NSIDC DAAC). A separate metadata file with an .xml file extension is also delivered to NSIDC DAAC with the HDF5 file; it contains the same information as the HDF5 file-level metadata.

A separate QA file with a `.qa` file extension is also associated with each data file. QA files are ASCII text files that contain statistical information in order to help users better assess the quality of the associated data file.

Various levels of QA are conducted with Level-1C data. If a product does not fail QA, it is ready to be used for higher-level processing, browse generation, active science QA, archive, and distribution. If a product fails QA, it is never delivered to NSIDC DAAC.

In addition, during the post-launch Calibration/Validation period, the performance of the Level-1C brightness temperature product relative to the Level-1B brightness temperature product was evaluated in a number of ways. These included:

- Comparing images and examining differences between the two products over coastlines and other discrete boundaries, and heterogeneous terrain (lakes, mountains, rivers).
- Comparing TB and TB-gradient histograms of the two products over regions of varying heterogeneity.

Refer to the Appendix for details on all data flags.

3 SOFTWARE AND TOOLS

For tools that work with SMAP data, refer to the Tools web page.

4 VERSION HISTORY

Table 4. Version History

Version	Date Implemented	Impacted Temporal Coverage	Description of Changes
v03.0	August 2020	31 March 2015 to 04 December 2023	Changes to this version include: • An improved calibration methodology was applied to the input Level-1B radiometer brightness temperatures. • The data algorithms, structure, content, or processor code are otherwise unchanged from the previous version.
v02.0	June 2018		Updated input SPL1BTB product with water correction applied, resulting in warmer TBs over land and cooler TBs over water.
v01.0	December 2016		First public data release

5 RELATED DATA SETS

SMAP Data at NSIDC | Overview

SMAP Radar Data at the ASF DAAC

6 RELATED WEBSITES

SMAP at NASA JPL

7 CONTACTS AND ACKNOWLEDGMENTS

M. Julian Chaubell, Steven Chan, R. Scott Dunbar, Simon Yueh

Jet Propulsion Laboratory

California Institute of Technology

Pasadena, CA

Jinzheng Peng

NASA Goddard Space Flight Center

Greenbelt, MD

8 REFERENCES

Backus, G. and F. Gilbert. 1970. Uniqueness in the inversion of inaccurate gross Earth data. *Phil. Trans. R. Soc. Lond.* A 1970(266):123-192. https://doi.org/10.1098/rsta.1970.0005.

Chakraborty, P., Misra, A., Misra, T., & Rana, S. S. 2008. Brightness Temperature Reconstruction Using BGI. *IEEE Transactions on Geoscience and Remote Sensing*, 46(6), 1768–1773. https://doi.org/10.1109/tgrs.2008.916082

Chan, S. and R. S. Dunbar. 2020. SMAP Enhanced Level 1C Radiometer Product Specification Document, Version 3.0, R17 Extended Mission Release. JPL D-56290, Jet Propulsion Laboratory, Pasadena, CA. (see PDF).

Chaubell, J. 2016. SMAP Algorithm Theoretical Basis Document (ATBD) Level-1B Enhancement Radiometer Data Product (L1B_TB_E). SMAP Project, JPL D-56287, Jet Propulsion Laboratory, Pasadena, CA. (see PDF)

Chaubell, J. 2018. SMAP Algorithm Theoretical Basis Document (ATBD) Level-1(B/C) Enhancement Radiometer Data Product, Rev B. SMAP Project, JPL D-56287, Jet Propulsion Laboratory, Pasadena, CA. (see PDF)

Farrar, M. R., & Smith, E. A. 1992. Spatial resolution enhancement of terrestrial features using deconvolved SSM/I microwave brightness temperatures. *IEEE Transactions on Geoscience and Remote Sensing*, 30(2), 349–355. https://doi.org/10.1109/36.134084

Long, D. G., & Brodzik, M. J. 2016. Optimum Image Formation for Spaceborne Microwave Radiometer Products. *IEEE Transactions on Geoscience and Remote Sensing*, 54(5), 2763–2779. https://doi.org/10.1109/tgrs.2015.2505677

Long, D. G., & Daum, D. L. 1998. Spatial resolution enhancement of SSM/I data. *IEEE Transactions on Geoscience and Remote Sensing*, 36(2), 407–417. https://doi.org/10.1109/36.662726

Migliaccio, M., & Gambardella, A. 2005. Microwave radiometer spatial resolution enhancement. *IEEE Transactions on Geoscience and Remote Sensing*, 43(5), 1159–1169. https://doi.org/10.1109/tgrs.2005.844099

Peng, J., S. Misra, S. Chan, J. Chaubell, R. Bindlish, A. Bringer, A. Colliander, G. De Amici, E. P. Dinnat, D. Hudson, T. Jackson, J. Johnson, D. Le Vine, T. Meissner, P. Mohammed, J. Piepmeier, D. Entekhabi, S. Yueh. 2020. SMAP Radiometer Brightness Temperature Calibration for the

L1B_TB, L1C_TB (Version 5), and L1C_TB_E (Version 3) Data Products. SMAP Project, Jet Propulsion Laboratory, Pasadena, CA. (see PDF).

Poe, G. A. 1990. Optimum interpolation of imaging microwave radiometer data. *IEEE Transactions on Geoscience and Remote Sensing*, 28(5), 800–810. https://doi.org/10.1109/36.58966

Robinson, W. D., Kummerow, C., & Olson, W. S. 1992. A technique for enhancing and matching the resolution of microwave measurements from the SSM/I instrument. *IEEE Transactions on Geoscience and Remote Sensing*, 30(3), 419–429. https://doi.org/10.1109/36.142920

Sethmann, R., Burns, B. A., & Heygster, G. C. 1994. Spatial resolution improvement of SSM/I data with image restoration techniques. *IEEE Transactions on Geoscience and Remote Sensing*, 32(6), 1144–1151. https://doi.org/10.1109/36.338362

Stogryn, A. 1978. Estimates of brightness temperatures from scanning radiometer data. *IEEE Transactions on Antennas and Propagation*, 26(5), 720–726. https://doi.org/10.1109/tap.1978.1141919

9 DOCUMENT INFORMATION

9.1 Publication Date

September 2020

9.2 Date Last Updated

December 2024

APPENDIX – DATA FIELDS

This appendix provides a description of all data fields within the *SMAP Enhanced L1C Radiometer Half-Orbit 9 km EASE-Grid Brightness Temperatures* product. The data are grouped in the following main HDF5 groups:

- Global_Projection
- North_Polar_Projection
- South_Polar_Projection
- Metadata

For a description of metadata fields for this product, refer to the Product Specification Document (Chan & Dunbar, 2020).

North, South, and Global Projections

Table A1 describes the data fields within the HDF5 group for each projection. Data are provided in three EASE-Grid 2.0 projections:

- Global (M9, or Midlatitude 9 km)
- North (N9, or North 9 km)
- South (S9, or South 9 km)

Within each group, the data are provided in fore-looking and aft-looking views. Data from the fore- and aft-look portions of the 360° antenna scan are provided separately in order to benefit radiometric analyses over regions where there is strong dependence of brightness temperature (TB) on viewing azimuth. Each set of looks contains brightness temperature observations, instrument viewing geometry information, and quality bit flags. The fore-looking set refers to information derived from the Level-1B brightness temperature observations acquired in the fore-looking portion of the scans when the antenna angle falls between -90 degrees and 90 degrees; the aft-looking set refers to information derived from the Level-1B brightness temperature observations acquired in the backward-looking portion of the scans. Only those cells that are covered by the swath for a given projection receive a valid data value.

Table A - 1. Data Fields for North_Polar_Projection, South_Polar_Projection, and Global_Projection

Azimuth Direction	Data Field Name	Type	Byte	Valid Min	Valid Max	Unit	Fill/Gap Values	Derivation Method*
N/A	cell_col (Global Cylindrical projection)	Uint16	2	1	963	N/A	65534	2
	cell_col (North/South Polar projection)	Uint16	2	1	499	N/A	65534	2
	cell_grid_surface_status	Uint16	2	0	1	N/A	65534	2
	cell_lat	Float32	4	-90.0	90.0	degree	65534	2
	cell_lon	Float32	4	-180.0	180.0	degree	65534	2
	cell_row (Global Cylindrical projection)	Uint16	2	1	405	N/A	65534	2
	cell_row (North/South Polar projection)	Uint16	2	1	499	N/A	65534	2
Fore-Looking Data Arrays	cell_antenna_scan_angle_fore	Float32	4	0.0	360.0	degree	-9999.0	1
	cell_boresight_incidence_fore	Float32	4	0.0	90.0	degree	-9999.0	1
	cell_centroid_lat_fore	Float32	4	-90.0	90.0	degree	-9999.0	1
	cell_centroid_lon_fore	Float32	4	-180.0	180.0	degree	-9999.0	1
	cell_number_measurements_3_fore	Uint16	2	1	N/A	N/A	65534	1
	cell_number_measurements_4_fore	Uint16	2	1	N/A	N/A	65534	1
	cell_number_measurements_h_fore	Uint16	2	1	65535	N/A	65534	1
	cell_number_measurements_v_fore	Uint16	2	1	65535	N/A	65534	1
	cell_solar_specular_phi_fore	Float32	4	0.0	360.0	degree	65534	1
	cell_solar_specular_theta_fore	Float32	4	0.0	90.0	degree	-9999.0	1
	cell_surface_water_fraction_mb_h_fore	Float32	4	0.0	1.0	N/A	-9999.0	1
	cell_surface_water_fraction_mb_v_fore	Float32	4	0.0	1.0	N/A	-9999.0	1
	cell_tb_3_fore	Float32	4	-50.0	50.0	K	-9999.0	1
	cell_tb_4_fore	Float32	4	-50.0	50.0	K	-9999.0	1
	cell_tb_error_3_fore	Float32	4	0.0	330.0	K	-9999.0	1
	cell_tb_error_4_fore	Float32	4	0.0	330.0	K	-9999.0	1
	cell_tb_error_h_fore	Float32	4	0.0	330.0	K	-9999.0	1
	cell_tb_error_v_fore	Float32	4	0.0	330.0	K	-9999.0	1

	cell_tb_h_fore	Float32	4	0.0	330.0	K	-9999.0	1
	cell_tb_h_surface_corrected_fore	Float32	4	0.0	330.0	K	-9999.0	1
	cell_tb_qual_flag_3_fore	Uint16	2	0	65,536	N/A	65534	1
	cell_tb_qual_flag_4_fore	Uint16	2	0	65,536	N/A	65534	1
	cell_tb_qual_flag_h_fore	Uint16	2	0	65,536	N/A	65534	1
	cell_tb_qual_flag_v_fore	Uint16	2	0	65,536	N/A	65534	1
	cell_tb_time_seconds_fore	Uint16	2	0	N/A	seconds	-9999.0	1
	cell_tb_time_utc_fore	Char24	2	2014-10-31 T00:00:00.000Z	N/A	N/A	N/A	1
	cell_tb_v_fore	Float32	4	0.0	330.0	K	-9999.0	1
	cell_tb_v_surface_corrected_fore	Float32	4	0.0	330.0	K	-9999.0	1
Aft-Looking Data Arrays	cell_antenna_scan_angle_aft	Float32	4	0.0	360.0	degree	-9999.0	1
	cell_boresight_incidence_aft	Float32	4	0.0	90.0	degree	-9999.0	1
	cell_centroid_lat_aft	Float32	4	-90.0	90.0	degree	-9999.0	1
	cell_centroid_lon_aft	Float32	4	-180.0	179.999	degree	-9999.0	1
	cell_number_measurements_3_aft	Uint16	2	1	N/A	N/A	65534	1
	cell_number_measurements_4_aft	Uint16	2	1	N/A	N/A	65534	1
	cell_number_measurements_h_aft	Uint16	2	1	65535	N/A	65534	1
	cell_number_measurements_v_aft	Uint16	2	1	65535	N/A	65534	1
	cell_solar_specular_phi_aft	Float32	4	0.0	360.0	degree	-9999.0	1
	cell_solar_specular_theta_aft	Float32	4	0.0	90.0	degree	-9999.0	1
	cell_surface_water_fraction_mb_h_aft	Float32	4	0.0	1.0	N/A	-9999.0	1
	cell_surface_water_fraction_mb_v_aft	Float32	4	0.0	1.0	N/A	-9999.0	1
	cell_tb_3_aft	Float32	4	-50.0	50.0	K	-9999.0	1
	cell_tb_4_aft	Float32	4	-50.0	50.0	K	-9999.0	1
	cell_tb_error_3_aft	Float32	4	0.0	330.0	K	-9999.0	1
	cell_tb_error_4_aft	Float32	4	0.0	330.0	K	-9999.0	1
	cell_tb_error_h_aft	Float32	4	0.0	330.0	K	-9999.0	1

	cell_tb_error_v_aft	Float32	4	0.0	330.0	K	-9999.0	1
	cell_tb_h_aft	Float32	4	0.0	330.0	K	-9999.0	1
	cell_tb_h_surface_corrected_aft	Float32	4	0.0	330.0	K	-9999.0	1
	cell_tb_qual_flag_3_aft	Uint16	2	0	65,536	N/A	-9999.0	1
	cell_tb_qual_flag_4_aft	Uint16	2	0	65,536	N/A	-9999.0	1
	cell_tb_qual_flag_h_aft	Uint16	2	0	65,536	N/A	-9999.0	1
	cell_tb_qual_flag_v_aft	Uint16	2	0	65,536	N/A	-9999.0	1
	cell_tb_time_seconds_aft	Float64	4	0	N/A	seconds	-9999.0	1
	cell_tb_time_utc_aft	Char24	2	2014-10-31T00:00:00.000Z	N/A	N/A	N/A	1
	cell_tb_v_aft	Float32	4	0.0	330.0	K	-9999.0	1
	cell_tb_v_surface_corrected_aft	Float32	4	0.0	330.0	K	-9999.0	1
	cell_tb_qual_flag_h_aft	Float32	4	0.0	330.0	K	-9999.0	1

*** Derivation methods are:**

1. From Level-1C brightness temperature data
2. From 36 km EASE-Grid 2.0 array definition
3. Value corrected for the presence of water wherever water/land areal fraction is below a threshold; when the fraction is zero, no correction is performed.
4. Determined by Level-2 soil moisture passive processing software
5. Available only with option algorithms that use two polarization channels
6. From external ancillary data whose location and timestamp coincide with those of the input data
7. From Level-2 soil moisture active data

Data Field Definitions

All data field definitions below are valid for fore-looking and aft-looking groups, as well as ascending and descending half-orbit files.

cell_col
EASE grid column index of cell on world grid in longitude direction.

cell_grid_surface_status
Indicates if the grid point lies on land (0) or water (1).

cell_lat
Latitude of the center of the Earth-based grid cell.

cell_lon
Longitude of the center of the Earth-based grid cell.

cell_row
EASE grid row index of cell on world grid in latitude direction.

cell_antenna_scan_angle fore|aft
Representative scan angle of the SMAP antenna on the spacecraft for all fore-/aft-looking footprints within the cell.

cell_boresight_incidence fore|aft
Representative angle between the antenna boresight vector and the normal to the Earth's surface for all fore-/aft-looking footprints within the cell.

cell_centroid_lat fore|aft
Weighted average of the latitude of the center of the fore-/aft-looking brightness temperature footprints that fall within the EASE-Grid cell.

cell_centroid_lon fore|aft
Weighted average of the longitude of the center of the fore-/aft-looking brightness temperature footprints that fall within the EASE-Grid cell.

cell_number_measurements_3 fore|aft
Number of fore-/aft-looking TB3 samples within the grid cell that were used to calculate the representative value in this product.

cell_number_measurements_4 fore|aft
Number of fore-/aft-looking TB4 samples within the grid cell that were used to calculate the representative value in this product.

cell_number_measurements_h fore|aft
Number of fore-/aft-looking TBH samples within grid cell that were used to calculate the representative value in this product.

cell_number_measurements_v fore|aft
Number of fore-/aft-looking TBV samples within grid cell that were used to calculate the representative value in this product.

cell_solar_specular_phi fore|aft
Weighted average of the azimuthal component of a spatial angle defined by the vector that extends from the sun to the solar glint spot and the antenna boresight vector for fore-/aft-looking footprints within the cell.

cell_solar_specular_theta fore|aft
Weighted average of the elevation component of the spatial angle defined by the vector that extends from the sun to the solar glint spot and the antenna boresight

vector for fore-/aft-looking footprints within the cell.

cell_surface_water_fraction_mb_h fore|aft
Gain-weighted fraction of static water within the fore-/aft-looking horizontally polarized antenna pattern.

cell_surface_water_fraction_mb_v fore|aft
Gain-weighted fraction of static water within the fore-/aft-looking vertically polarized antenna pattern.

cell_tb_3 fore|aft
Representative TB3 for all fore-/aft-looking samples that fall within the grid cell.

cell_tb_4 fore|aft
Representative TB4 for all fore-/aft-looking samples that fall within the grid cell.

cell_tb_error_3 fore|aft
Error measure of the representative TB3 for all fore-/aft-looking samples that fall within the grid cell.

cell_tb_error_4 fore|aft
Error measure of the representative TB4 for all fore-/aft-looking samples that fall within the grid cell.

cell_tb_error_h fore|aft
Error measure of the representative TBH for all fore-/aft-looking samples that fall within the grid cell.

cell_tb_error_v fore|aft
Error measure of the representative TBV for all fore-/aft-looking samples that fall within the grid cell.

cell_tb_h fore|aft
Representative TBH for all fore-/aft-looking samples that fall within the grid cell.

cell_tb_h_surface_corrected fore|aft
Water/land contamination corrected fore-/aft-looking horizontally polarized brightness temperature at the surface after RFI filtering within the grid cell.

cell_tb_qual_flag_3 fore|aft
Bit flags that represent the quality of the fore-/aft-looking 3rd Stokes brightness temperature for each grid cell. Refer to Table A - 2.

cell_tb_qual_flag_4 fore|aft
Bit flags that represent the quality of the fore-/aft-looking 4th Stokes brightness temperature for each grid cell. Refer to Table A - 2.

cell_tb_qual_flag_h fore|aft
Bit flags that represent the quality of the fore-/aft-looking horizontal polarization brightness temperature within each grid cell. Refer to Table A - 2.

cell_tb_qual_flag_v fore|aft
Bit flags that represent the quality of the fore-/aft-looking vertical polarization brightness temperature within each grid cell. Refer to Table A - 2.

cell_tb_time_seconds fore|aft
Weighted average of the acquisition time of all of the fore-/aft-looking brightness temperature footprints with a center that falls within the EASE-Grid cell in seconds since noon on January 1, 2000 UTC.

cell_tb_time_utc fore|aft
ASCII representation of the weighted average of the acquisition time of all of the fore-/aft-looking brightness temperature

footprints with a center that falls within the EASE-Grid cell in UTC.

cell_tb_v fore|aft
Representative TBV for all fore-/aft-looking samples that fall within the grid cell.

cell_tb_v_surface_corrected fore|aft
Water/land contamination corrected fore-/aft-looking vertically polarized brightness temperature at the surface after RFI filtering within the grid cell.

Table A - 2. Bit Values for all Cell TB Quality Flags (TH, TV, T3, and T4)

Bit Position	Bit Value and Interpretation
0	0 = Has acceptable quality
	1 = Does not have acceptable quality
1	0 = Within expected range
	1 = Beyond expected range
2	0 = RFI not detected
	1 = RFI detected
3	0 = RFI detected and corrected (RFI algorithm functioned correctly; however, does not indicate that resultant bit is RFI free)
	1 = RFI was detected but not correctable in the observation
4	0 = Has acceptable NEDT
	1 = Has unacceptable NEDT
5	0 = Solar direct TB correction successful
	1 = Solar direct TB correction not successful
6	0 = Solar specular TB correction successful
	1 = Solar specular TB correction not successful
7	0 = Lunar specular TB correction successful
	1 = Lunar specular TB correction not successful
8	0 = Galactic specular TB correction successful
	1 = Galactic specular TB correction not successful
9	0 = Atmospheric correction successful
	1 = Atmospheric correction not successful
10	0 = Faraday rotation correction successful
	1 = Faraday rotation correction not successful
11	0 = Faraday rotation correction was successful
	1 = Faraday rotation correction was not successful
12	0 = The corresponding brightness temperature element contains a calculated value
	1 = The corresponding brightness temperature element is null

Bit Position	Bit Value and Interpretation
13	0 = Observation was within half orbit
	1 = Observation was outside half orbit
14	0 = The difference between TA filtered and TA is less than the threshold
	1 = The difference between TA filtered and TA is not less than the threshold
15	0 = Radiometer processor declares a pixel is free of RFI by incorporating the following factors: • The data are in range (Bit 1) • The RFI removal algorithm worked (Bit 3) • The data do not display high NEDT (Bit 4) • The difference between TA filtered and TA is less than a specific threshold (Bit 14)
	1 = Radiometer processor does not declare a pixel is free of RFI

Fill/Gap Values

SMAP data products employ fill and gap values to indicate when no valid data appear in a particular data element. Fill values ensure that data elements retain the correct shape. Gap values locate portions of a data stream that do not appear in the output data file.

Fill values appear in the SMAP enhanced Level-1C brightness temperature product when the enhanced Level-1C brightness temperature Science Production Software (SPS) can process some, but not all, of the input data for a particular swath grid cell. Fill data may appear in the product in any of the following circumstances:

- One of SPS executables that generate the SMAP enhanced Level-1C brightness temperature product is unable to calculate a particular science or engineering data value. The algorithm encounters an error. The error disables generation of valid output. The SPS reports a fill value instead.
- Some of the required science or engineering algorithmic input are missing. Data over the region that contributes to particular grid cell may appear in only some of the input data streams. Since data are valuable, the enhanced Level-1C brightness temperature product records any outcome that can be calculated with the available input. Missing data appear as fill values.
- Non-essential information is missing from the input data stream. The lack of non-essential information does not impair the algorithm from generating needed output. The missing data appear as fill values.
- Fill values appear in the input radiometer the Level-1B brightness temperature product. If only some of the input that contributes to a particular grid cell is fill data, the enhanced Level-1C brightness temperature SPS will most likely be able to generate some output. However, some portion of the enhanced Level-1C brightness temperature output for that grid cell may appear as fill values.

SMAP data products employ a specific set of data values to connote that an element is fill. The selected values that represent fill are dependent on the data type.

No valid value in the enhanced Level-1C brightness temperature product is equal to the values that represent fill. If any exceptions should exist in the future, the enhanced Level-1C brightness temperature content will provide a means for users to discern between elements that contain fill and elements that contain genuine data values. This document will also contain a description of the method used to ascertain which elements are fill and which elements are genuine.

The enhanced Level-1C brightness temperature product records gaps in the product level metadata. The following conditions will indicate that no gaps appear in the data product:

- Only one instance of the attributes *Extent/rangeBeginningDateTime* and *Extent/rangeEndingDateTime* will appear in the product metadata.
- The character string stored in metadata element *Extent/rangeBeginningDateTime* will match the character string stored in metadata element *OrbitMeasuredLocation/halfOrbitStartDateTime*.
- The character string stored in metadata element *Extent/rangeEndingDateTime* will match the character string stored in metadata element *OrbitMeasuredLocation/halfOrbitStopDateTime*.

One of two conditions will indicate that gaps appear in the data product:

- The time period covered between *Extent/rangeBeginningDateTime* and *Extent/RangeEndingDateTime* does not cover the entire half orbit as specified in *OrbitMeasuredLocation/halfOrbitStartDateTime* and *OrbitMeasuredLocation/halfOrbitStartDateTime*.
- More than one pair of *Extent/rangeBeginningDateTime* and *Extent/rangeEndingDateTime* appears in the data product. Time periods within the time span of the half orbit that do not fall within the sets of *Extent/rangeBeginningDateTime* and *Extent/rangeEndingDateTime* constitute data gaps.

Acronyms and Abbreviations

Table A - 3. Acronyms and Abbreviations

Abbreviation	Definition
ABFCS	Antenna Beam Frame Coordinate System
Char	8-bit character
Int8	8-bit (1-byte) signed integer
Int16	16-bit (2-byte) signed integer
Int32	32-bit (4-byte) signed integer
ECR	Earth Centered Rotating
ET	Ephemeris Time
Float32	32-bit (4-byte) floating-point integer
Float64	64-bit (8-byte) floating-point integer
H-pol	Horizontally polarized
N/A	Not Applicable
NEDT	Noise Equivalent Delta Temperature
PRI	Pulse Repetition Interval
RFI	Radio Frequency Interference
SI	International System of Units
SPS	Science Production Software
SRF	Science Orbit Reference Frame
TA	Antenna Temperature
TB	Brightness Temperature
Uint8	8-bit (1-byte) unsigned integer
Uint16	16-bit (2-byte) unsigned integer
UTC	Universal Coordinated Time
V-pol	Vertically polarized